Antenna Loading by Passive Impedance for Linear-to-Circular Polarization Conversion

Luis Felipe Fonseca Dias, Camille Jouvaud, Christophe Delaveaud, Hervé Aubert

Linear-to-Circular Polarization Conversion of the Electromagnetic Field from Wireless Tags

Luis Felipe Fonseca-Dias, *Student Member, IEEE*, Camille Jouvaud, Christophe Delaveaud, *Member, IEEE*, and Hervé Aubert, *Senior Member, IEEE*

***Abstract*—Many passive and wireless devices, such as RFID tags or batteryless wireless sensors, are designed to control electromagnetic field backscattered by the devices, in order to maximize the interrogation range (or the device-to-reader separation distance) and/or to mitigate the electromagnetic clutter. In this Letter, we show that a linearly-polarized electromagnetic field can be converted into a circularly-polarized field by using a passive and chipless device. The device, also called tag, consists of a one-port antenna loaded by a passive impedance, whose value is derived from a rigorous electromagnetic model including structural and antenna scattering modes. The experimental validation of predicted Linear-to-Circular polarization conversion is reported in the case of a patch antenna illuminated by a linearly-polarized field. At the operating frequency of 2.6 GHz, the measured axial ratio of the electric field backscattered by the tag is lower than 1 dB.**

***Index Terms*— electromagnetic scattering from antennas, field polarization, Radar Cross Section measurement.**

I. Introduction

The control of the electromagnetic field backscattered by antennas has been studied for decades [1]-[5]. Widely applied to low-cost wireless communication systems, such control allows maximizing the interrogation range (or the device-to-reader separation distance) and mitigating the electromagnetic clutter in RFID systems or in wireless sensor networks **Erreur ! Source du renvoi introuvable.**-[8]. Compared with standard wireless systems in which tags backscatter a Linearly-Polarized (LP) electromagnetic field (i.e., when the LP-to-LP conversion is performed by tags), the measured interrogation range is actually increased by 17% when a Circularly-Polarized (CP) field when illuminated by a CP field (i.e., the CP-to-CP conversion is performed by tags)[9]. Moreover, CP antennas may be advantageously used to mitigate the line-of-sight clutter in wireless indoor communication applications [10]. In addition, when tags convert an incident LP electromagnetic field into a backscattered cross-polarized field, the interrogation range may reach 50 m [11]. Depolarizing tags can be also used to compensate [12] or take advantage [13] of the misalignment between chipless RFID tags and the reader. Using high-impedance surfaces [14], ultrawideband LP-to-CP conversion has been demonstrated for both Right-Handed or Left-Handed CP for a single design with increased interrogation performance [15]. In this approach, the scatterers/reflectors are designed to optimize their structural scattering behavior in terms of the polarization.

Authors of the present study proposed recently to achieve the LP-to-CP conversion from a tag, which consists of a singleport antenna loaded by a passive impedance [16], [17], by control of its antenna scattering mode. For the first time, we report here the experimental validation of LP-to-CP conversion by using wireless tags. The tags consist of a one-port patch antenna loaded by a passive impedance, whose value allows converting a LP incident electromagnetic field into a CP backscattered field. Such impedance is derived from a rigorous electromagnetic model including the structural and antenna scattering modes.

The Letter is organized as follows. In Section II, we report the electromagnetic scattering model used to derive the value of the impedance to be used for loading a one-port antenna and achieving LP-to-CP conversion. We show that passive impedances can be selected to obtain such polarization conversion. The experimental validation of the theoretically predicted LP-to-CP conversion is reported in Section III.

II. Theoretical Derivation of the Load Impedance of One-Port Antennas for LP-to-CP Conversion

This Letter investigates the electromagnetic scattering of a tag composed of single-port antenna, which is loaded by a passive impedance. From the scattering model based on the Norton equivalent circuit[3], the Authors have previously derived the co- and cross-polarized components of the electromagnetic field backscattered by single-port antennas, when illuminated by a linearly-polarized electromagnetic field [16]. The vertically- and horizontally-polarized (VP and HP) components of the electric field backscattered by the tag in the direction (θ_s, ϕ_s), denoted respectively by E_s^v and E_s^h, are given as follows:

$$\begin{cases} E_s^v(\alpha_i, Z_L) = E_0^v(\alpha_i) - \frac{Z_L}{Z_L + Z_a} A^v(\alpha_i) \\ E_s^h(\alpha_i) = E_0^h(\alpha_i) \end{cases} \quad (1)$$

where Z_L denotes the (complex) impedance used to load the single-port antenna of input impedance Z_a, and α_i is the slant

Manuscript received XXX; revised XXX; accepted XXX. Date of publication XXX.

L. F. Fonseca-Dias, C. Jouvaud and C. Delaveaud are with the Laboratory of Antennas, Propagation and Inductive Coupling, CEA Leti, Grenoble 38054, France (e-mail: luisfelipe.fonsecadias@cea.fr; camille.jouvaud@cea.fr; christophe.delaveaud@cea.fr).

H. Aubert is with the Laboratory of Analysis and Systems Architecture, CNRS, Toulouse 31000, France (e-mail: herve.aubert@laas.fr).

angle of linearly-polarized electric field incident upon the antenna, E_0^v and E_0^h are respectively the VP and HP components of the backscattered electric field in the direction (θ_s, ϕ_s) when the antenna input port is short-circuited. Let $I_0(\alpha_i)$ be the current flowing in the short-circuit for the given slant angle α_i. In (1), $A^v(\alpha_i)$ is then defined as follows:

$$A^v(\alpha_i) = \frac{I_0(\alpha_i)}{I_a} E_{ant}^v \quad (2)$$

where E_{ant}^v is the VP component of the electric field radiated by the antenna in the direction (θ_s, ϕ_s), when the current I_a is impressed at the input port of the antenna. From (1) and (2), it can be derived that the load impedance Z_L^+ (resp. Z_L^-) required to backscatter a left-handed (resp. right-handed) circularly-polarized field in the direction (θ_s, ϕ_s) for the slant angle α_i is given by:

$$Z_L^{\pm} = \frac{Z_a}{\frac{A^v}{E_0^v \pm j\, E_0^h} - 1} \quad (3)$$

where $j^2 = -1$. Consequently, the computation of $Z_L^{\pm}$ requires the knowledge of the VP E_0^v and HP E_0^h components of the backscattered electric field in the direction (θ_s, ϕ_s) and the knowledge of the contribution A^v in this direction. However, the direct determination of E_0^v, E_0^h and A^v from measurement is often difficult in practice. For instance, the measurement accuracy of the structural scattering mode contribution E_0^v strongly depends on the quality (over the frequency band of interest) of the short-circuit impedance used to shunt the antenna, especially for antennas having an electrically large ground plane. In addition, characterizing the contribution of the antenna scattering mode A^v from (2) requires the knowledge of the currents I_0 and I_a, whose derivation from measurement is not straightforward at high frequencies. To overcome practical issues, we propose here to determine E_0^v as well as A^v from the measurement of any two VP components E_1^v and E_2^v of the electromagnetic field backscattered by the antenna, when its input port is loaded by known (but non-zero) distinct impedances Z_1 and Z_2, respectively. According to (1), we can actually obtain E_0^v and A^v from E_1^v and E_2^v, as follows:

$$E_0^v(\alpha_i) = E_1^v + \frac{Z_1}{Z_1 + Z_a} A^v(\alpha_i) \quad (4\text{-a})$$

$$A^v(\alpha_i) = 2\frac{(1-\Gamma\Gamma_1)(1-\Gamma\Gamma_2)}{(1-\Gamma^2)(\Gamma_1-\Gamma_2)}[E_2^v(\alpha_i) - E_1^v(\alpha_i)] \quad (4\text{-b})$$

where Γ is the reflection coefficient at the input port of the antenna, while Γ_1 and Γ_2 are the reflection coefficients at the impedances Z_1 and Z_2, respectively. Consequently, neither the currents I_a and I_0 nor the radiating field E_{ant}^v are needed to derive E_0^v and A^v from (4). If Z_1 is set to zero ($\Gamma_1 = -1$) and Z_2 is set to infinite ($\Gamma_2 = +1$), (4-b) reduces to:

$$A^v(\alpha_i) = -[E_s^v(\alpha_i, +\infty) - E_S^v(\alpha_i, 0)] \quad (5\text{-a})$$

$$= E_0^v(\alpha_i) - E_s^v(\alpha_i, +\infty) \quad (5\text{-b})$$

In order to avoid the implementation of power supply in tags, only passive impedances $Z_L^{\pm}$ given by (3) are of interest in this study.

III. Experimental Validation of the LP-to-CP Conversion

A. Material and methods

In this section, we report the first experimental results on the LP-to-CP conversion from the impedance loading of a rectangular patch antenna operating at 2.45 GHz. The patch antenna and passive load impedance are shown in Fig. 1. The measured reflection coefficient at the antenna input port is of -34 dB at 2.45 GHz, the measured antenna gain is of 8 dBi, and the cross-polarization discrimination is higher than 30 dB in the broadside direction. The LP-to-CP conversion achieved by the patch antenna loaded by the impedance $Z_L^{\pm}$ derived from (3) is characterized in an anechoic chamber by using identical transmitting (T_X) and receiving (R_X) horn antennas (about 10 dBi of gain in the frequency band of interest). The experimental configuration is bistatic, as the T_X- and R_X-antennas are not in the same position. The Tx-antenna is VP, while the orientation of the Rx-antenna is mechanically controlled to measure, for any slant angle α_i of the incident LP electric field, the two-orthogonal components E_s^v and E_s^h of the electric field backscattered by the loaded antenna. The impedance-loaded antenna is called here the *Scatterer Under Test* (SUT). The SUT, Tx- and Rx-antennas are positioned at the height of 1.52 m above the floor of the anechoic chamber. The separation distance between the T_X-antenna and R_X-antenna is of 0.8 m (6.5λ), while the distance between these two antennas and SUT is of 3.48 m. Moreover, the electric field transmitted by the T_X-antenna is normally incident upon the SUT planar surface, and the bistatic angle is of 13°. The SUT backing is composed of a fixed plastic base to monitor the 2D orientation of SUT, and it is placed in a foam support, as shown in Fig. 2. A hollowed plastic disk is used to hold the SUT and control the slant angle, measured at a 6° step from 0° to 90° (or Horizontal to Vertical Incident polarization).

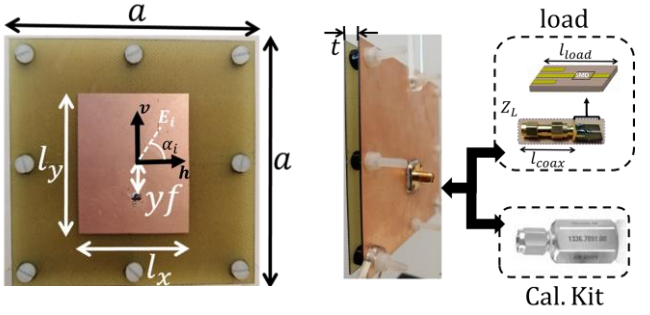

(a) (b)

Fig. 1. (a) Front view of the rectangular patch antenna operating at 2.45 GHz with relative slant angle α_i to the incident field E_i) (l_y = 0.37λ, l_x = 0.29λ, a = 0.65λ, y_f = 0.09λ, t_{subs} = 0.0065λ and t_{air} = 0.04λ, where λ = 122.45 mm and relative permittivity of the substrate εs_{ubs} = 4.3); (b) Profile view showing the antenna input port connected to either the open-ended microstrip line with a series Surface Mount Device (SMD) resistor (l_{load} = 0.08λ) and the coaxial connector (l_{coax} = 0.21λ) to connect the load impedance, and the Calibration Kit loads

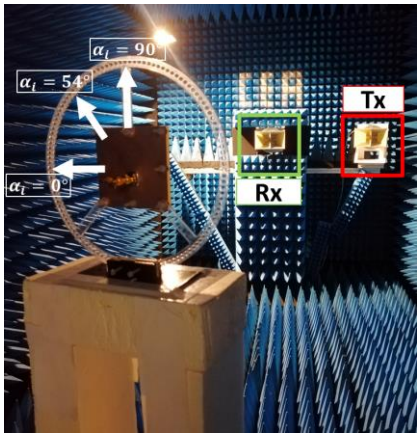

Fig. 2. Experimental setup in the anechoic chamber using identical horn (T_X- and R_X-) antennas and the impedance-loaded patch antenna (SUT) placed on the plastic disk over a foam support. The white arrows indicate the relative slant angle α_i between the SUT and Tx-antenna as the disk is turned.

The experimental instrument setup based on Vector Network Analyser (VNA) offers a tunable measurement bandwidth from 1.5 GHz to 6 GHz, with a frequency step of 1 MHz. The total number of field measurement is then of 9002 per slant angle and load impedance. The setup is calibrated by using a simplified model, based on the polarimetric technique reported in [16] and named *Single-Reference Calibration* [17]. Following [18], this calibration is applied to our bistatic configuration. When the SUT is illuminated by a linearly (vertically or horizontally) polarized electric field, the measured cross-polarization discrimination of the patch antenna is found to be larger than 20 dB in the direction of the R_X-antenna. Compared with the magnitude of the co-polarized component of the backscattered electric field, the cross-polarized component can then be neglected. For this reason, only one metallic sphere is required to calibrate the polarization measurement setup [17,19]. Finally, in order to mitigate the impact on measurement results of multiple electromagnetic reflections, we apply the time gating approach proposed in [16].

B. Determination of the passive load impedance to achieve the LP-to-CP conversion

We characterize the contribution of both the structural and antenna scattering modes to the total electromagnetic field backscattered by the impedance-loaded patch antenna in the arbitrary direction defined by $\theta_s = 0°$ and $\phi_s = 13°$. The position of the load is illustrated in Fig. 1b. From (4-b) we first derive A^v in this direction from the measurement of the VP components E_1^v and E_2^v of the electric field backscattered by the antenna, when its input port is loaded respectively by the short-circuit Z_1 (SC) and open-circuit Z_2 (OC) of the R&S ZV-Z235 calibration kit ($Z_1 = 0.1 + j25.6\ \Omega$ and $Z_2 = 0.03 - j97.5\ \Omega$ @ 2.45 GHz). The impedances $Z_1$and $Z_2$of the R&S ZV-Z235 calibration kit are not ideal short-circuit (Z_1 is not zero) and ideal open-circuit (Z_2 is not infinite) impedances. However, as $Z_1 \cong Z_0^2/Z_2$ (where $Z_0 = 50\ \Omega$), they can be used to calibrate the VNA (see, e.g., [20]). Next, the electric field E_0^v is derived from (4-a) and using (1), the electric field backscattered by the patch antenna loaded by any passive impedance Z_L can be finally estimated from A^v and E_0^v.

Fig. 3 displays the estimated magnitude of the electric field backscattered at 2.615 GHz (i.e., the frequency which centers the Left-Handed CP region) in the direction ($\theta_s = 0°, \phi_s = 13°$) by the antenna as a function of the load impedance Z_L and the slant angle of 54°, that is, the angle for which the lowest axial ratio is achieved. Lines along which the axial ratio keeps the same value are indicated in yellow in Fig. 3. It can be observed that a good trade-off between a low Axial Ratio and high field magnitude can be found. At 2.615 GHz, the impedance Z_L^{CP}=102.6 + j115.3 Ω offers actually a good compromise, as it can be observed from Fig. 3. As expected from (3), when it is loaded by this passive impedance, the patch antenna backscatters a left-handed circularly-polarized electric field at the frequency of 2.615 GHz predicted by the electromagnetic simulations (see Fig. 4 and 5).

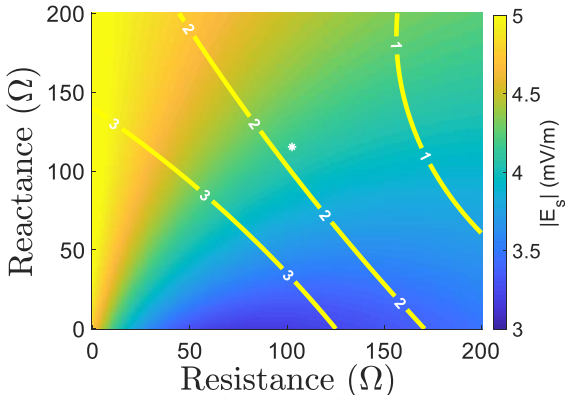

Fig. 3. Estimated magnitude of the electric field backscattered by the patch antenna of Fig. 2 as a function of the resistance and reactance of the passive impedance Z_L connected at the input port of the antenna. The magnitude is derived from (1) by the using components of scattering modes E_0^v and A^v, estimated from (4), in the direction ($\theta_s = 0°, \phi_s = 13°$) at 2.615 GHz and for incident slant angle α_i of 54°. Along the yellow solid lines, the axial ratio is the same and equals to 1, 2 or 3.

C. Experimental validation of the LP-to-CP conversion

For the patch antenna loaded by the passive impedance Z_L^{CP} derived in Section III.B, a good agreement is obtained in Fig. 5 between the axial ratios derived from measurement, full-wave electromagnetic simulation (CST MWS) and the electromagnetic model reported in Section II.

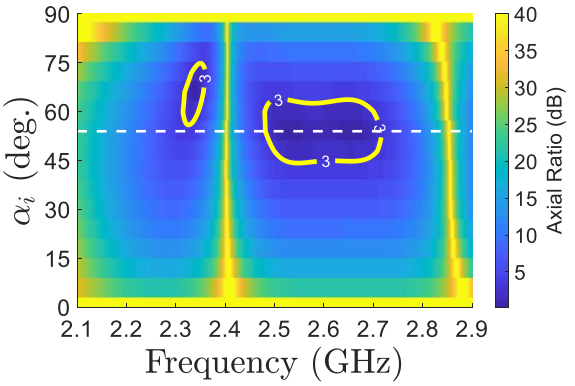

Fig. 4. Measured Axial Ratio as a function of both frequency and slant angle α_i with a 6° step (the yellow contours indicate the regions where the axial ratio is lower than 3 dB and the dashed white line highlights the axial ratio in function of frequency at a fixed slant angle $\alpha_i = 54°$)

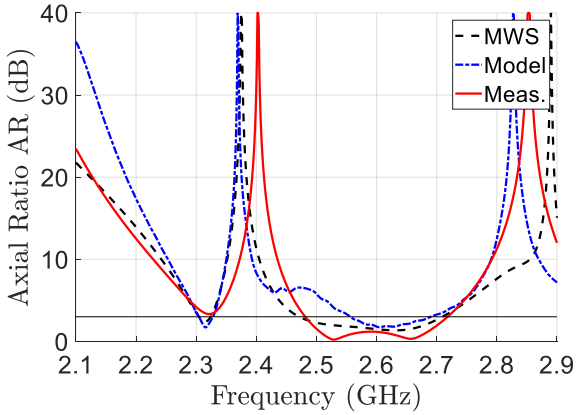

Fig. 5. Axial Ratio, as function of frequency at fixed $\alpha_i = 54°$, obtained from: full-wave electromagnetic simulation (CST MWS, black dashed curve), the electromagnetic model of Section II (blue dotted curve) and direct measurements (red solid curve).

Moreover, we observe in Fig. 4 and 5 two frequency bands in which the CP is obtained: (1) the Right-Handed CP is achieved in a very small bandwidth (< 1%) at a frequency lower than the antenna operating frequency (2.315 GHz), and (2) the Left-Handed CP is generated in a larger bandwidth of around 9% centered at a frequency higher than the antenna operating frequency (that is, between 2.48 GHz and 2.70 GHz). In these two frequency bands, the frequencies at which the measured Axial Ratio reached its highest magnitude (at 2.4 and 2.85 GHz, respectively) are very close (<1%) to those predicted by full-wave simulations and the electromagnetic model presented in Section II.

IV. Conclusion

We have experimentally validated a scattering model to design passive tags that convert a Linearly-Polarized incident electromagnetic field into a Circularly-Polarized backscattered field. We have demonstrated the existence of passive impedances for achieving such polarization conversion. Future work will be focused on investigating the interrogation range in the presence of line-of-sight clutter.

References

[1] R. B. Green, "The General Theory of Antenna Scattering," ElectroScience Laboratory, Columbus, OH, Report No. 1223-17, 30 Nov. 1963.

[2] R. Harrington, "Theory of loaded scatterers," Proc. *IEEE*, vol. 111, No. 4, pp. 617–623, April 1964.

[3] R. C. Hansen, "Relationships between antennas as scatterers and as radiators,", *Proc. IEEE*, Vol. 77, No. 5, pp. 659-662, May 1989.

[4] R. E. Collin, "Limitations of the Thévenin and Norton Equivalent Circuits for a Receiving Antenna," *IEEE Ant. & Propag. Magazine*, Vol. 45, No. 2, pp. 119-124, June 2003

[5] W. Wiesbeck and E. Heidrich, "Wide-band multiport antenna characterization by polarimetric RCS measurements," *IEEE Trans. on Ant. & Propag.*, Vol. 46, No. 3, pp. 341-350, Mar. 1998.

[6] K. Rao, P. Nikitin, and S. Lam, "Antenna design for UHF RFID tags: a review and a practical application," *IEEE Trans. on Ant. & Propag.*, vol. 53, no. 12, pp. 3870–3876, Dec. 2005.

[7] B. S. Cook, R. Vyas, S. Kim, T. Thai, T. Le, A. Traille, H. Aubert, and M. M. Tentzeris, "RFID-Based Sensors for Zero-Power Autonomous Wireless Sensor Networks," *IEEE Sensors Journal*, vol. 14, no. 8, pp. 2419–2431, Aug. 2014.

[8] T. T. Thai, H. Aubert, P. Pons, G. DeJean, M. M. Tentzeris, and R. Plana, "Novel Design of a Highly Sensitive RF Strain Transducer for Passive and Remote Sensing in Two Dimensions," *IEEE Trans. on Microw. Theory & Techn.*, vol. 61, no. 3, pp. 1385–1396, Mar. 2013.

[9] J. Garc´ıa, A. Arriola, F. Casado, X. Chen, J. I. Sancho, and D. Valderas, "Coverage and read range comparison of linearly and circularly polarised radio frequency identification ultra-high frequency tag antennas," *IET Microwaves, Ant. & Propag.*, vol. 6, no. 9, pp. 1070–1078, Jun. 2012.

[10] T. Rappaport and D. Hawbaker, "Wide-band microwave propagation parameters using circular and linear polarized antennas for indoor wireless channels," *IEEE Trans. on Communications*, vol. 40, no. 2, pp. 240–245, Feb. 1992.

[11] D. Henry, J. G. D. Hester, H. Aubert, P. Pons, and M. M. Tentzeris, "Long-Range Wireless Interrogation of Passive Humidity Sensors Using Van-Atta Cross-Polarization Effect and Different Beam Scanning Techniques," *IEEE Trans. on Microw. Theory & Techn.*, vol. 65, no. 12, pp. 5345–5354, Dec. 2017.

[12] F. Costa, S. Genovesi, and A. Monorchio, "Chipless RFIDs for Metallic Objects by Using Cross Polarization Encoding," *IEEE Trans. on Ant. & Propag.*, vol. 62, no. 8, pp. 4402–4407, Aug. 2014.

[13] T. Marchal, J. Philippe, D. Henry, M. V. De Paolis, A. Coustou, P. Pons, and H. Aubert, "Millimetre-Wave Interrogation of Passive Sensors Embedded Inside Closed Reverberant Environments from DualPolarized Passive Repeaters," in *2019 49th Euro. Microw. Conf. (EuMC)*, Oct. 2019, pp. 33–36.

[14] E. Doumanis, G. Goussetis, J. L. Gomez-Tornero, R. Cahill, and V. Fusco, "Anisotropic impedance surfaces for linear to circular polarization conversion," *IEEE Trans. on Ant. & Propag.*, vol. 60, no. 1, pp. 212–219, Jan. 2012.

[15] S. Genovesi, F. Costa, F. A. Dicandia, M. Borgese, and G. Manara, "Orientation-insensitive and normalization-free reading chipless rfid system based on circular polarization interrogation," *IEEE Trans. on Ant. & Propag.*, vol. 68, no. 3, pp. 2370–2378, Mar. 2020.

[16] L. F. Fonseca Dias, C. Jouvaud, C. Delaveaud, and H. Aubert, "Linearto-Circular Polarization Conversion from Impedance Loading of SinglePort Patch Antennas," in 2020 IEEE Inter. Symp. on Ant. & Propag. (ISAP) and N.A. Radio Science Meeting, Jul. 2020, pp. 1119–1120, iSSN: 1947-1491.

[17] L. F. Fonseca-Dias, C. Jouvaud, C. Delaveaud and H. Aubert, "Polarization Conversion from a Two-Port Impedance Loaded Tag," in 2022 *49th Euro. Conf. on Ant. & Propag. (EuCAP)*, Madrid, Spain, Mar. 2022.

[18] W. Wiesbeck and S. Riegger, "A complete error model for free space polarimetric measurements," *IEEE Trans. on Ant. & Propag.*, vol. 39, no. 8, pp. 1105–1111, Aug. 1991.

[19] W. Wiesbeck and D. Kahny, "Single reference, three target calibration and error correction for monostatic, polarimetric free space measurements," Proc. of the IEEE, vol. 79, no. 10, pp. 1551–1558, Oct. 1991.

[20] D. Kahny, K. Schmitt, and W. Wiesbeck, "Calibration of bistatic polarimetric radar systems," *IEEE Trans. on Geoscience & Remote Sensing*, Vol. 30, No. 5, Sep 1992.

[21] G. T. Ruck, D. E. Barrick, W. D. Stuart, and C. K. Krichbaum, *Radar Cross Section Handbook*, Vol. 1. New York: Plenum Press, 1970.

[22] M. Hiebel, *Fundamentals of Vector Network Analysis*, Rohde & Schwarz, 2007.